Computational Analysis of Flow in a Curved Tube Model of the Coronary Arteries: Effects of Time-varying Curvature

ALAND SANTAMARINA,* ERLEND WEYDAHL,* JOHN M. SIEGEL, JR.,[†] and JAMES E. MOORE, JR.*

*Mechanical Engineering Department, Florida International University, Miami, FL, and [†]CFD Research Corporation, Huntsville, AL

Abstract—The flow through a curved tube whose radius of curvature varies with time was studied in order to better understand flow patterns in coronary arteries. A computational flow model was constructed using commercially available software. The artery model featured a uniform circular cross section, and the curvature was assumed to be constant along the tube, and in one plane. The computational model was verified with the use of a dynamically similar *in vitro* apparatus. A steady uniform velocity was prescribed at the entrance at a Reynolds number of 300. Two sets of results were obtained: one in which the curvature was held constant at the mean, maximum and minimum radii of curvature (quasistatic), and another in which the curvature was varied sinusoidally in time at a frequency of 1 Hz (dynamic). The results of the dynamic analysis showed that the wall shear rates varied as much as 52% of the static mean wall shear rate within a region of 10 tube diameters from the inlet. The results of the dynamic analysis were within 6% of the quasistatic predictions. Realistic modeling of the deforming geometry is important in determining which locations in the coronary arteries are subjected to low and oscillating wall shear stresses, flow patterns that have been associated with atherogenesis. © *1998 Biomedical Engineering Society.* [S0090-6964(98)00306-3]

INTRODUCTION

Statistics show that atherosclerosis is the leading cause of death in western countries. Various factors such as high blood pressure, high blood cholesterol levels, cigarette smoking, diabetes, obesity, family history and a sedentary lifestyle are indicative of an individual's risk of developing atherosclerosis.[1] However, none of these factors can explain why the disease develops only in certain arteries because their effects are felt throughout the cardiovascular system. The vessels most commonly affected are the abdominal aorta, femoral, carotid, and coronary arteries.

Address correspondence to Dr. James E. Moore, Jr., Florida International University, Mechanical Engineering Department, Miami, FL 33199. Electronic mail: James@eng.fiu.edu

The highly localized nature of atherosclerosis has led to the hypothesis that mechanical factors, such as blood flow patterns, may be involved in its formation. Much research has been devoted to identify more specifically the mechanical conditions that lead to atherosclerosis formation. In particular, low mean and oscillating fluid wall shear stresses have been shown to correlate with specific locations of intimal thickening in the carotid artery[14] and in the abdominal aorta.[20]

An important site of atherosclerosis formation is the coronary arteries. If coronary atherosclerosis progresses to the point where the flow to the distal heart tissue is limited, a myocardial infarction often results. Approximately 66% of all atherosclerosis-related medical and loss of productivity costs are attributed to the formation of the disease in the coronary arteries.[1]

Despite their obvious importance, comparatively less is known about the details of flow in the coronary arteries than in the carotid artery and the aorta. Batten and Nerem[3] measured velocity profiles in a representative static curved bifurcation model of the left main coronary artery and found that the velocity profiles were skewed toward the inner wall of curvature and toward the inner walls of the bifurcation. Sabbah *et al.*[27] constructed a static flow model based on a cast of a postmortem porcine specimen. Their flow visualization results indicated helical flow patterns that arose due to the secondary flow for both steady and pulsatile flow. Mark *et al.*[19] demonstrated the importance of taking pulsatility into account when modeling coronary flow. Their model, based on a cast of a human coronary artery, was later used to obtain wall shear stress measurements which were correlated with intimal thickness data.[9] A negative correlation was noted between intimal thickness and both mean and maximum shear stress. Tang *et al.*[32] constructed a curved bifurcation model of the left main coronary artery based on average measurements of human casts. They noted that the velocity profile was skewed toward the outer wall of curvature, and toward the inner walls of the bifurcation. A three-dimensional (3D) pulsatile, compu-

tational analysis of a static model of a coronary artery branch showed that the degree of wall shear stress oscillation was generally smaller than that found in the carotid and abdominal aorta.[13] Additionally, the branch angle of the bifurcation (the angle between the left anterior descending and left circumflex arteries) was given values of 0°, 48° and 90°. The velocity profiles in the left anterior descending and left circumflex arteries were skewed toward the inner walls of the bifurcation regardless of the bifurcation angle, and the degree of skewness was not greatly affected by the bifurcation angle.

All of these studies indicate that the spatial variation in wall shear stress in the coronary arteries is predominantly determined by the vessel geometry. The coronary arteries are curved as they traverse around the myocardium, with additional, varying degrees of curvature in the plane of the myocardial surface. The diameter of the left main coronary artery is approximately 4 mm,[9,25] with the left anterior descending and circumflex arteries exhibiting diameters of approximately 3 mm.[13] The curvature ratio (δ=vessel radius/radius of curvature=a/R) in the left coronary artery tree varies greatly depending on the particular location, but usually lies in the range of 0.02–0.5.[11,13,18,25] An additional implication of the curvature associated with the coronary arteries is that their geometry varies dynamically due to the contraction of the myocardium. The total displacement of the coronary arteries can be separated into a solid-bodylike movement and a deformation. Moore et al.[21] showed that the movement in an obtuse marginal branch of the left circumflex coronary artery is as much as five times the vessel diameter. The deformation that is relevant to the present study is the change in curvature. The change in curvature may be expressed by a deformation parameter ε, defined as the ratio

$$\varepsilon = \frac{\Delta R}{R_{\text{mean}}}, \qquad (1)$$

where ΔR is the amplitude of the change in radius of curvature and R_{mean} is the mean radius of curvature. Pao et al.[23] measured that radius of curvature of the left anterior descending coronary artery at the first diagonal branch over a full cardiac cycle. Taking R_{mean} as the average of the maximum and minimum values, their results show ε=0.8. Gross et al.[11] made similar measurements in the left anterior descending artery approximately 3 cm distal to the third diagonal, and found ε =0.7. Smaller values of ε were noted in other anatomic locations. Unfortunately, the effects of dynamic physiologic movement and deformation due to the contraction of the heart on coronary artery blood flow have not received much attention in the literature. Studies have been published on the effects of axial[21] and lateral[7]

movement on flow in the coronary arteries, but the vessels were assumed to remain straight during the movement.

The effects of curvature on flow in circular tubes have been the topic of many studies, as summarized in Pedley[24] and in Berger et al.[4] The characterizing parameters for flow in a curved tube are the mean curvature ratio (δ_m=tube radius/mean radius of curvature =a/R_{mean}) and the Dean number (κ). The Dean number is a ratio of the product of inertia and centrifugal forces to the viscous forces, and may be defined as $\delta_m^{1/2}$ Re, where Re is the Reynolds number based on the average velocity and the tube diameter. There are other definitions of κ found in the literature, most notably those that involve the pressure gradient rather than the average velocity.[24] In this study, the Reynolds number is held constant, while different values of δ_m are investigated. Therefore, δ_m and the Reynolds number will be used for reference purposes rather than the Dean number. Because of the centrifugal effects the flow in a curve tube will skew toward the outer wall. The inner wall is therefore a location of relatively low wall shear stress, and in some arteries, a common location of intimal thickening.

The coronary arteries represent a unique curved tube flow situation because their curvature varies with time. In most previous studies of flow in the coronary arteries (e.g., Refs. 13, 25, and 32), the curvature was assumed to be constant. It has not yet been determined if physiologic changes in curvature are important in determining wall shear stress patterns in the coronary arteries. A preliminary in vitro study analyzed the effects of dynamic curvature changes.[29] In that study, a flexible curved tube was placed in a moving carriage assembly and the radius of curvature was changed sinusoidally in time and held constant in space. The curvature was uniplanar, and the cross sectional area of the tube was maintained constant. A steady pressure gradient and a fully developed inlet velocity profile were prescribed. The Reynolds number was Re=540, and the Womersley parameter of the deformation was α=9. In this case, the Womersley parameter is defined by

$$\alpha = a \sqrt{\frac{\omega}{\nu}}, \qquad (2)$$

where ω is the angular frequency of the deformation and ν is the fluid kinematic viscosity. The mean curvature ratio was δ_m=0.035 and the two deformation parameters employed were ε=0.07 and ε=0.15. Pulsed Doppler ultrasound was used to measure the velocity profile. As expected from static curved tube models, the velocity profile was skewed toward the outer wall. The change in the maximum velocity was as much as 13% of the average flow velocity, and there was a shift in the location

of the point of maximum velocity. This maximum variation occurred when the radius of curvature was in transition from the minimum to its maximum value. Conversely, there was only a 3% difference in the velocity profiles measured in a stationary tube held at the minimum and the maximum radii of curvature. That study, although limited in the values employed for curvature ratio and deformation parameter, clearly showed that the velocity profile depends on the instantaneous dynamic vessel movement.

The governing flow equations for a bending tube were derived by Lynch *et al.*[18] They included an approximate, perturbation-type solution to these equations for the case when the curvature in a weakly curved tube (small δ_m) is varying slightly (small ε) at a low frequency (small α). The effects of time-dependent curvature on the wall shear stress amplitude were found to be on the order of 10^{-3} compared to the effects of the presence of curvature itself. The change in mean wall shear stress was predicted to be on the order of 10^{-7}. Their solution predicted a higher mean axial wall shear stress at the inner and outer walls of curvature due to the appearance of a steady streaming term. At the midwall (halfway between the inner and outer walls along the circumference), the mean shear was predicted to decrease. The dynamic effects on the mean shear stress were predicted to follow the square of the arc length away from a point in the tube that remains fixed. Although their results showed dynamic effects on the mean azimuthal wall shear stress, this term vanished at the inner, mid and outer walls.

Another recent study measured dynamic coronary artery flexion angiographically, and tracked the narrowing of the coronary arteries over a period of approximately two years.[31] Although the focus of that study was on the mechanical stresses within the arterial walls, the angiography data showed a statistically significant correlation between higher degrees of cyclic flexion and plaque advancement. The mean flexion angle (defined by the change in the slope of the tangent to the vessel from systole to diastole) at stenoses that showed significant advancement was 19°, as opposed to 9° for stenoses that showed no advancement.

The goal of this study is to begin to analyze the effects of physiologic time-varying curvature on velocity profiles and wall shear rates in a simplified model of the coronary arteries. The primary purpose of this article is to present the development of the computational methodology, including verification by an *in vitro* flow apparatus, and present results when the radius of curvature of a simplified coronary artery model is varied with a sinusoidal wave form at a base cardiac frequency of 1 Hz. Although the parameters used in the construction of this model are physiologic, the geometry has been simplified

so that a basic understanding of the fluid mechanics may be obtained.

METHODS

Computational Model

This study employed computational techniques to solve the full three-dimensional, unsteady Navier-Stokes equations for blood flow through a curved tube simulating a typical section of the coronary artery tree. Computational fluid dynamics (CFD) techniques have emerged as a powerful tool to study hemodynamics in complex physiologic geometries. Compared with experimental methods, CFD can more easily accommodate user-defined variations in arterial anatomy and flow wave form. The computational solutions yield velocities at all points within the artery and can provide wall shear rates (WSRs) with high accuracy at all surfaces.

The model geometry used for this study was based on the second model described by Tang *et al.*,[32] as well as data compiled from several other sources as mentioned in the Introduction.[9,11–13,18,21–23,25] The curvature in this model was assumed to be uniplanar and constant over the entire length of the tube at any instant. The entry to the tube was kept fixed at all times, thus the location of the center of curvature varied with time. The variation in curvature was specified as a sinusoidal function, specifically, $R(t) = R_{\mathrm{mean}}[1 + \varepsilon \cos(\omega t)]$. The tube was assumed to maintain a circular cross section with a constant diameter. Nine different simulations were run. Three values of δ_m were employed, 0.03, 0.08 and 0.12. Three different values of ε were used, 0.1, 0.3 and 0.5. The Reynolds number was 300, and the Womersley parameter of the deformation was 1.88 for all cases. The Dean numbers for each of the cases $\delta_m = 0.03$, 0.08 and 0.12 were 52, 85 and 104, respectively. The inlet velocity profile was flat (plug flow) and steady. The fluid was assumed to be incompressible, homogeneous, and Newtonian. These assumptions have been shown to be reasonable for general arterial hemodynamics studies by several previous investigators (e.g., Refs. 10 and 26).

The boundary conditions included no slip at the tube wall (fluid velocity at the tube wall = tube wall velocity) and symmetry about the diameter located in the curvature plane. The symmetry assumption was used so that the flow field would have to be solved in only one-half of the tube cross section (Fig. 1). A constant pressure condition was applied at the outlet. In the interpretation of the results, the portion of the tube near the exit was not included. For the $\delta_m = 0.03$ simulations, the total tube length was 32 tube diameters (TDs), but only the results from the first 25 TDs are shown. For the $\delta_m = 0.08$ simulations, the first 15 TDs of a total tube length of 19.3 TDs are shown, and for $\delta_m = 0.12$, the first 10 TDs of a total tube length of 12.3 TDs are shown. Shorter tubes
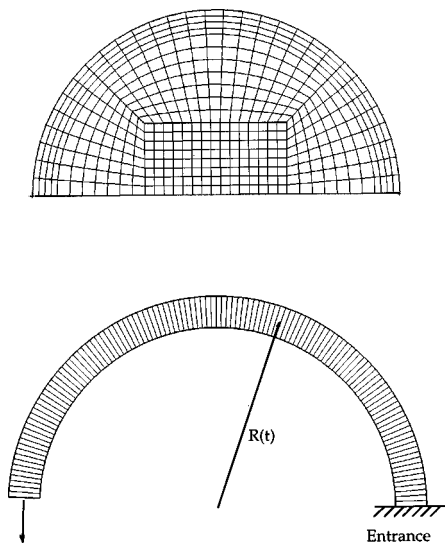
FIGURE 1. Cross sectional and longitudinal views of the computational mesh used in the computational calculations. The entrance was kept fixed during the deformation of the tube.

were used for higher δ_m because the tube would have closed on itself at the entry if the tube were longer. There are two reasons for not showing the data near the end of the tubes. First, no one segment of the coronary vasculature retains its uniplanar curvature for a very long length due to the continual presence of branches or changes in curvature. No results beyond 10 TDs should be considered as directly relevant to flow in the coronary arteries, although more results are shown here for reference purposes. A second reason was to minimize the effects of the constant pressure condition at the exit on the proximal flow patterns. These effects were limited to within approximately 1 TD of the exit, based on visual inspection of the shear rate data.

The code used for this study was based on a finite volume method. The flow domain was discretized using a body fitted, structured grid. The computational fluid dynamics software used was CDF-ACE (CFD Research Corp., Huntsville, AL). Computational flow simulations of this type are based on the division of the flow domain into small (finite) volumes. Finite volume techniques enforce mass and momentum conservation through the integration of the governing flow equations over a given finite volume. The equations from all of the volumes in a flow field are then linearized and combined to produce algebraic relationships that are solved numerically. For these simulations, the grid was required to move according to the prescribed deformation parameter ε. An arbitrary Lagrangian-Eulerian approach was used to implement the grid movement into the solution code. In this approach, a space conservation law was introduced that was de-coupled from the flow governing equations due

to the prescribed deformation. This methodology has been validated for other moving grid problems using CFD-ACE.[15,16] The flow calculations were performed on a Silicon Graphics Power Challenge computer server located at the Florida International University Engineering Information Center. A typical run time for one flow case was two weeks per cycle of full time use of a single processor. The results were transferred back to a Silicon Graphics Indy Workstation for postprocessing and viewing.

A typical finite volume mesh is illustrated in Fig. 1. In the cross section, near the tube wall, there is a finer clustering of cells to achieve sufficient resolution to accurately compute the wall shear rate. A total of 461 cells was used in the cross section. Along the length of the tube, the number of cells depended on δ_m and ε. However, the largest cell dimension in the axial direction was 0.66 TD. The simulated cardiac cycle was divided into 1000 time steps. In order to verify that a solution was grid and time step independent, the grid size was doubled until the WSR results were within 3% of the previous solution. Similarly, the time step was decreased by a factor of 2 until the WSR results were within 3% of the previous solution. These are highly selective thresholds for grid and time step insensitivity because they are based on the first spatial derivative of a flow quantity, rather than on a flow quantity itself. These tests were conducted at an axial position of 8 TDs where the flow would have been fully developed in a static tube,[2] and at $t=0.4$, for $\delta_m=0.08$ and $\varepsilon=0.5$. The process for the mesh generation was divided into two steps: the generation of the mesh itself and the deformation of the mesh. The first step was accomplished using the tools available in the pre-processing software, CFD-GEOM. The second step was accomplished by writing a customized subroutine that was linked with the solver.[28] This subroutine took sufficient information from CFD-ACE regarding each node (initial position, time, time step) and returned the new position based on the radius of curvature function. Each simulation was begun with the tube at the maximum radius of curvature, and with fluid velocities from a static simulation of the tube at the maximum radius of curvature. Periodicity was confirmed by allowing the simulation to run for more than two cycles and comparing the velocities from successive cycles. The differences were less than 1% after one cycle.

Two sets of simulations were run. The first was a quasistatic analysis in which the curvature was held constant at the mean, maximum and minimum radii of curvature. These simulations were run in order to ascertain the differences in the flow field that result from just the fact that the geometry changes. In the second set of simulations, the curvature was varied dynamically as described above. The comparison of the two sets of simu-

lations should reveal the importance of the fact that the curvature is varying dynamically.

The results were displayed as axial velocity profiles, velocity vectors and wall shear rates for interpretation. The wall shear rate in this case expresses contributions from all components of the shear rate tensor. However, the axial wall shear rate is expected to dominate over the azimuthal contribution along most of the wall. At the inner and outer walls, the azimuthal component of wall shear rate is zero by symmetry.

The interpretation of the results was aided by defining a normalized wall shear rate amplitude (NWSRA). The amplitude in wall shear rate for the dynamic case was expressed as the difference between the maximum and minimum wall shear rate values at each axial position. For the quasistatic case, the amplitude was taken to be the difference between the wall shear rates at the static maximum and minimum radii of curvature. These values were then normalized with respect to the static WSR at the mean radius of curvature at each axial position to obtain the NWSRA (Fig. 5).

Experimental Verification

The computational model was verified by constructing an *in vitro* experimental flow apparatus. A specific case with geometrical and flow parameters that could be produced experimentally was simulated with the computational model. Using the same grid employed for all cases described in the computational section, the results were compared with the experimental data. The geometrical parameters used in the experiment (and duplicated in a separate computational simulation) were $\delta_m = 0.043$, $\varepsilon = 0.26$, Re$=300$, and $\alpha = 4.2$. A long straight section (30 cm or 23 tube diameters) of nonmoving tubing preceded the curved tube, producing fully developed (Poiseuille) flow conditions at the entry. A fully developed entry condition was used because a flat entry profile would have been very difficult to produce reliably at the entrance to a moving tube (with all of its associated hardware). An additional computational simulation with a fully developed entry profile was run to correspond as closely as possible to the experimental case.

The curved section of the tube consisted of a 1.27 cm inside diameter platinum-cured silicone rubber tube, surrounded by a spiral vacuum hose to prevent distortion of the silicone tube's cross section during deformation. The deformation was produced by a motor coupled through a crank-piston linkage to a carriage that slides on two hardened-steel rails (Fig. 2). The crank-piston linkage converts rotational motion to linear motion in a near sinusoidal wave form.[28] The resulting wave form was input to the computational model in order to match the motion. The tube was clamped to a bar suspended from the moving carriage. The direction of motion of the bar
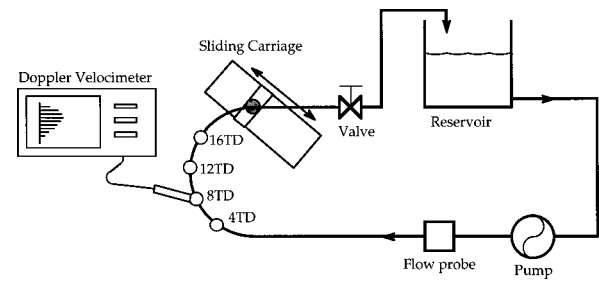
FIGURE 2. Illustration of the experimental flow apparatus used to confirm the computational results. The measurement locations are marked.

was such that the inlet to the curved section remained fixed. The working fluid was a water-glycerin solution of 65% glycerin by volume with a kinematic viscosity of 0.12 cm²/s. One gram of cornstarch per liter of fluid was added for ultrasonic signal reflection.

An Ismatec standard drive pump (Ismatec S.A., Zurich, Switzerland) provided a stable, steady flow rate. The volume flow rate was measured using a Transonic Systems transit time ultrasonic flowmeter (Transonic Systems Inc., Ithaca, NY) that was calibrated using a graduated cylinder and a stopwatch. The velocity profiles along the diameter connecting the inner and outer walls of curvature were measured at locations approximately 4, 8, 12 and 16 tube diameters from the inlet to the curved tube section using pulsed Doppler ultrasound (Fig. 2). A DOP1000 high resolution pulsed Doppler ultrasound velocimeter (Signal Processing S.A., Lausanne, Switzerland) was used to measure the fluid velocities, with an emitted frequency of 4 MHz. The sample volume size was 3.6 mm (window of 2 μs and assuming a speed of sound of 1820 m/s). In order to facilitate the comparison, the computationally calculated velocities were projected to the probe axis. Thus, the velocities shown in Fig. 9 are not purely in the axial direction. The experimental data were acquired for 20 simulated cardiac cycles, each triggered by the movement of the tube, and ensemble averaged. The standard deviations of the 20 samples at each location are given in Fig. 9. An additional calibration was performed by measuring the flow in the straight tube entry section and multiplying the experimental values by a constant correction factor to match the theoretical parabolic profile.

RESULTS

A computational study of the flow patterns in a curved tube with dynamic varying curvature showed that within the first 10 TDs from the entrance, the flow development is similar to a static curved tube with the same mean curvature. The following is a physical description of the instantaneous axial and cross sectional
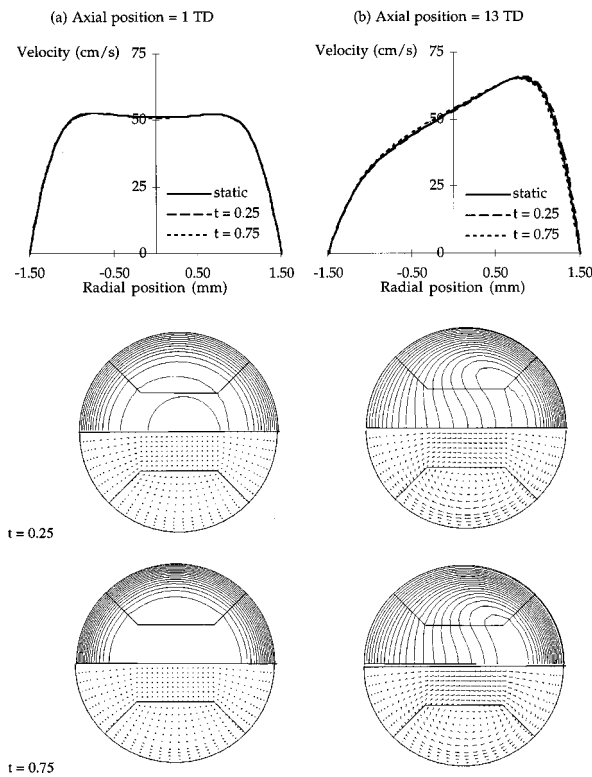
FIGURE 3. Axial velocity profiles, contour plots and secondary flow vector fields of the computational results at axial positions (a) 1 TD from the inlet and (b) 13 TDs from the inlet. The static (mean radius of curvature) and dynamic results are shown for time points $t=0.25$ and $t=0.75$. At these time points, the instantaneous radius of curvature is equal to the mean radius of curvature.

FIGURE 4. Wall shear rate vs normalized axial position at the inner and outer walls for the static (mean radius of curvature) and dynamic cases at the same two time points shown in Fig. 3. For reference, the shear rate in an equivalent, fully developed, straight tube flow would be 1067 s^{-1}.

flow patterns with a Reynolds number of 300 (the only value used in this study), a mean curvature of $\delta_m=0.08$ and a deformation parameter $\varepsilon=0.5$ at time points $t=0.25$ and $t=0.75$. The radius of curvature is equal to the mean value at both time points, decreasing at $t=0.25$ and increasing at $t=0.75$. The flow patterns observed at other values of δ_m and ε were similar to those described here. Near the inlet, the flow is dominated by the developing boundary layer with an inviscid core, much like flow development in a straight pipe. At 1 TD from the inlet [Fig. 3(a)], the axial velocity is slightly skewed toward the inner wall, as was demonstrated by Singh[30] for static curved tubes. Further downstream, the axial velocity is accelerated by boundary layer displacement, thus increasing centrifugal forces in the core. The centrifugal effects become larger as the peak velocity increases, and begin to dominate over the effects of boundary layer growth, causing an outward skewing of the axial velocity [Fig. 3(b)]. Secondary flow in the cross sectional plane in the form of two symmetric vortices typical of curved tube flow was also observed, with fluid moving from the outer wall toward the inner wall along

the tube wall, and back to the outer wall through the core [Figs. 3(a) and 3(b)]. The inward/outward skewing of the velocity profile is also apparent in the shear rate plots for these cases (Fig. 4). At the outer wall, the WSR at $t=0.75$ is slightly higher than the static value or the value at $t=0.25$. Between 0 and 10 TDs the maximum deviation from the static results is 1.8% at the outer wall. Beyond 10 TDs there is an increase in the WSR at the outer wall, with a maximum deviation from the static results of 4% at 17 TDs. This indicates that the outer wall shear rate is greater when the radius of curvature is decreasing. The dynamic wall shear rate at the inner wall was also greater than the static case at this time, but the differences at all axial positions were very small (less than 2.5%).

The effects of dynamic curvature variation on the mean wall shear rate were revealed by comparing the time-averaged wall shear rate for the fully dynamic case to the wall shear rate in a static tube with a curvature ratio of δ_m. This provides an estimate of the error in the mean shear rate that results from assuming a static geometry. The mean wall shear rates at the inner and midwalls were always higher for the dynamic case. For $\delta_m=0.12$, $\varepsilon=0.5$, the inner wall mean shear rate was 6% higher at an axial position of 5.1 TDs (Fig. 5). The mean dynamic wall shear rate at the midwall for the same flow situation was 6.7% higher than the static value at 2.8 TDs (Table 1). The differences were smaller for the smaller values of δ_m, and for smaller values of ε. At the outer wall, the mean wall shear rate for the dynamic case was larger than the static value near the entry of the tube, then smaller for some portion, then again larger further downstream (Table 1). The differences at the outer wall were smaller in magnitude than the differences at the inner or midwalls. In all cases and at all
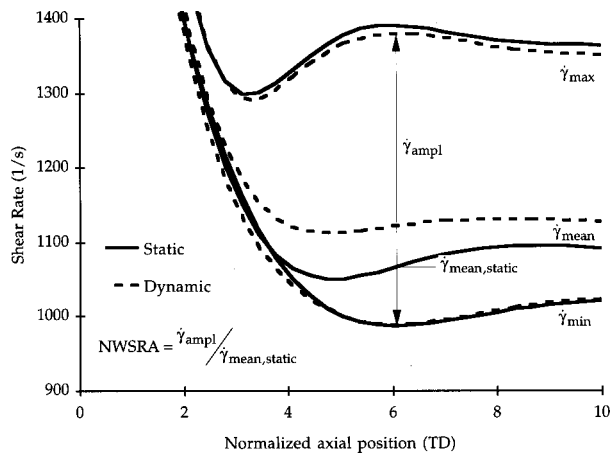
FIGURE 5. Wall shear rate vs axial position at the inner wall for $\delta_m = 0.12$ and $\varepsilon = 0.5$. The mean wall shear rate in the dynamic case for δ_m is the time-averaged wall shear rate, and was higher than the shear rate at the static mean radius of curvature. For reference, the shear rate in an equivalent, fully developed, straight tube flow would be 1067 s^{-1}. The normalized wall shear rate amplitude is defined as the difference between the maximum and minimum dynamic shear rates divided by the local shear rate at the static mean curvature.

locations, the maximum values occurred closer to the tube entrance for larger values of ε. The differences in the mean wall shear rate were 1.5% or less for the $\varepsilon = 0.1$ cases.

Analysis of quasistatic and dynamic wall shear rates over the entire simulated cardiac cycle revealed significant shear rate amplitudes caused by changes in curvature. At the inner and midwall locations, the largest NWSRA seen along the tube axis increased with increasing δ_m, and were largest for $\varepsilon = 0.5$. The following data

TABLE 1. Largest differences between the time-averaged (mean) wall shear rate for the dynamic case ($\varepsilon = 0.5$) and the wall shear rate in a static tube with a curvature ratio of δ_m. The axial positions where these differences occurred are given in parentheses. A positive value indicates a higher mean dynamic wall shear rate. At the outer wall, three local maxima occurred. These numbers represent the error in estimating the mean wall shear stress associated with assuming a static geometry.

	Inner wall	Midwall	Outer wall
$\delta_m = 0.03$	1.5% (10.1 TD)	3.3% (6.9 TD)	2.4% (4.9 TD)
			−1.0% (12.1 TD)
			0.12% (22.6 TD)
$\delta_m = 0.08$	3.3% (6.3 TD)	5.2% (3.5 TD)	1.4% (3.7 TD)
			−1.5% (7.1 TD)
			2.0% (13.5 TD)
$\delta_m = 0.12$	6.0% (5.1 TD)	6.7% (2.8 TD)	1.2% (2.8 TD)
			−1.5% (5.7 TD)
			2.3% (10.6 TD)

TABLE 2. Maximum normalized wall shear rate amplitudes (NWSRAs) for the dynamic cases. The axial positions at which the maximum NWSRA occurred are given in parentheses. The maximum NWSRA increases with δ_m and ε at the inner and midwalls. At the outer wall, the NWSRA increases with ε, but decreases with δ_m. The NWSRA occurs further upstream for larger values of ε.

	Inner wall	Midwall	Outer wall
$\delta_m = 0.03$			
$\varepsilon = 0.1$	2% (5.0 TD)	5% (10.3 TD)	5% (7.0 TD)
$\varepsilon = 0.3$	5% (4.8 TD)	15% (9.9 TD)	17% (4.7 TD)
$\varepsilon = 0.5$	7% (4.9 TD)	28% (9.5 TD)	28% (6.2 TD)
$\delta_m = 0.08$			
$\varepsilon = 0.1$	3% (8.1 TD)	7% (4.9 TD)	4% (4.7 TD)
$\varepsilon = 0.3$	9% (7.9 TD)	23% (4.9 TD)	13% (4.6 TD)
$\varepsilon = 0.5$	19% (7.6 TD)	44% (4.5 TD)	21% (4.3 TD)
$\delta_m = 0.12$			
$\varepsilon = 0.1$	5% (6.6 TD)	9% (3.7 TD)	4% (3.7 TD)
$\varepsilon = 0.3$	17% (6.4 TD)	28% (3.5 TD)	10% (3.8 TD)
$\varepsilon = 0.5$	37% (6.1 TD)	52% (3.1 TD)	19% (3.4 TD)

are for the $\varepsilon = 0.5$ dynamic cases, while the largest NWSRA for the other cases are given in Table 2. In the cases where the NWSRA diverged toward the end of the tube (such as occurs for $\delta_m = 0.03$, midwall; Fig. 6), the maximum value was taken to be the first local maximum. The largest variation in inner wall shear rate for $\delta_m = 0.03$ was NWSRA = 7%, occurring at an axial position of 4.9 TDs (Fig. 6). For $\delta_m = 0.08$, the largest NWSRA at the inner wall was 19%, occurring at 7.6 TDs (Fig. 7), and for $\delta_m = 0.12$, 37%, occurring at 6.1 TDs (Fig. 8). The greatest NWSRA were observed at the midwalls. The largest NWSRA at the midwalls were 26% for $\delta_m = 0.03$ (Fig. 6), 43% for $\delta_m = 0.08$ (Fig. 7), and 52% for $\delta_m = 0.12$ (Fig. 8). The maximum values occurred closer to the entrance for larger values of δ_m. At the outer wall, the NWSRA diminished with increasing δ_m,
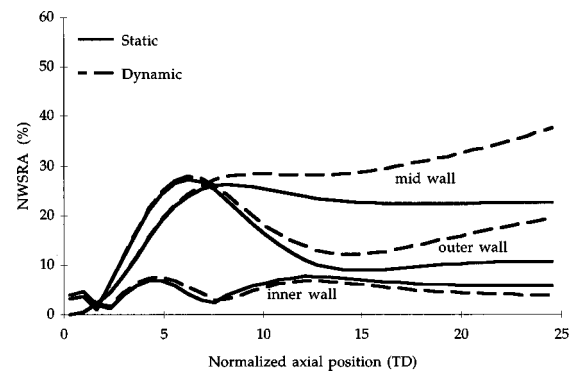
FIGURE 6. NWSRA vs axial position for $\delta_m = 0.03$ and $\varepsilon = 0.5$ at the inner, mid and outer walls. The NWSRA is higher at the mid and outer walls. The dynamic and quasistatic predictions were approximately the same within the first 10 TDs.
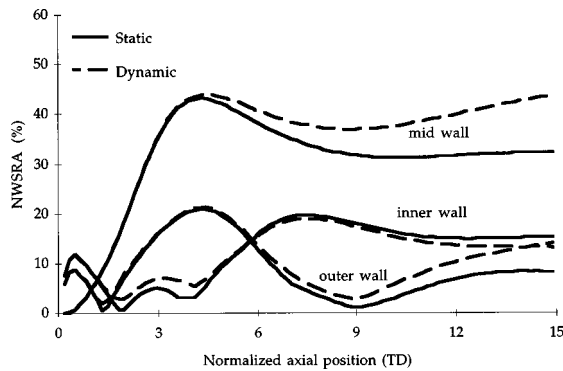
FIGURE 7. NWSRA vs axial position for $\delta_m=0.08$ and $\varepsilon=0.5$ at the inner, mid and outer walls. The NWSRA is higher at the midwall. The dynamic and quasistatic predictions were approximately the same within the first 10 TDs.

but still increased with ε. The largest NWSRA were 28% for $\delta_m=0.03$, 21% for $\delta_m=0.08$ and 19% for $\delta_m=0.12$ (Figs. 6–8 and Table 2). As was the case at the midwall, the maximum values occurred closer to the entrance for larger values of δ_m. Note that the outer wall NWSRA is larger than the inner wall NWSRA for $\delta_m=0.03$, but the opposite is true for $\delta_m=0.08$ and $\delta_m=0.12$. There was less shear rate variation due to curvature change at the outer walls of the more tightly curved tubes. In general, the maximum values occurred closer to the entrance for larger values of ε. The exception is the inner wall, for the case $\delta_m=0.03$ and $\varepsilon=0.1$, where the maximum values all occurred at approximately 5 TDs.

A comparison of the dynamic shear rate amplitudes to the variations noted in the quasistatic analysis demonstrated that the addition of dynamically varying curvature did not have a large effect less than 10 TDs from the inlet. In all cases, the NWSRA predicted by the dynamic analysis was within 6% of the variation predicted quasi-
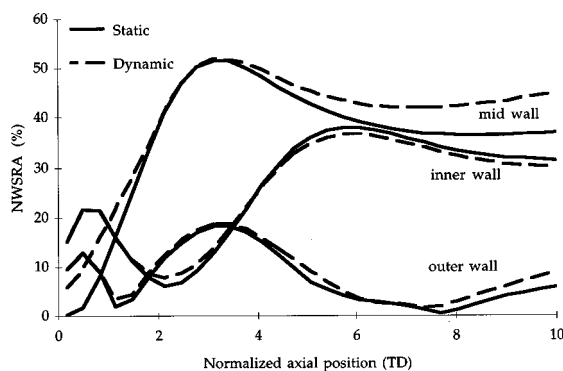
FIGURE 8. NWSRA vs axial position for $\delta_m=0.12$ and $\varepsilon=0.5$ at the inner, mid and outer walls. The NWSRA is higher at the inner and midwalls. The highest NWSRA noted in this study, 52%, was found at the midwall in this case. The dynamic and quasistatic predictions were approximately the same within the first 10 TDs.

(a) t = 0.28, axial position 4 TD   (b) t = 0.73, axial position 4 TD

(c) t = 0.28, axial position 16 TD   (d) t = 0.73, axial position 16 TD
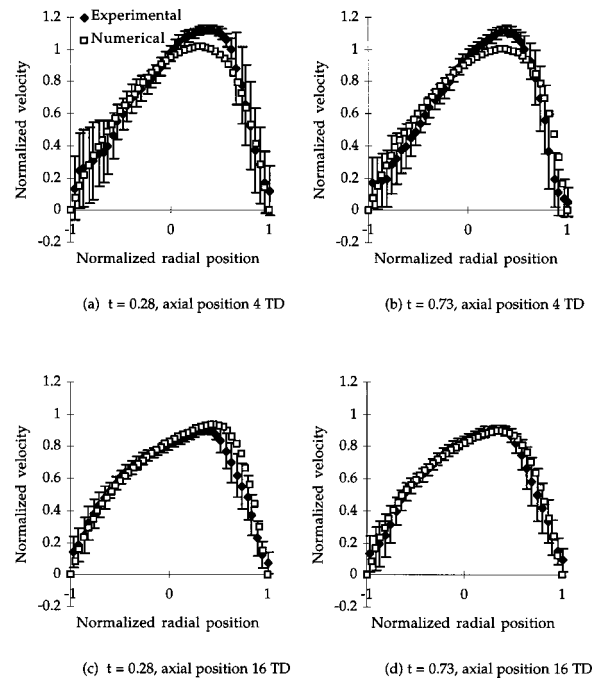
FIGURE 9. Comparison of the experimental and computational velocity profiles at (a) and (b) 4 TDs and (c) and (d) 16 TDs at two different time points in the simulated cardiac cycle. The correlation coefficient that resulted from comparing the experimental to the computational results at all positions and time points was 0.93.

statically (Figs. 6–8). However, larger differences of as much as 15% exist downstream (more than 10 diameters from the entry) for the midwall at $\delta_m=0.03$ and $\delta_m=0.08$ (Figs. 6 and 7).

A comparison of the experimentally measured velocity profiles corresponded well with the computational predictions. At an axial position of 4 TDs, $t=0.28$ [Fig. 9(a)], the peak experimental velocities were approximately 11% higher than the computational values. The peak velocities in both cases occurred at a normalized radial position of $+0.38$. Note also that the standard deviations of the experimental measurements are higher near the tube walls, in particular near the far tube wall (inner wall of curvature, radial position$=-1$). This is most likely due to echoes coming from the tube walls. At the same position and $t=0.73$, the peak experimental velocity was 11% higher than the computational value, with the peak velocities occurring at normalized radial positions of $+0.38$ for the experimental and $+0.36$ for the computational [Fig. 9(b)]. Further downstream, at 16 TDs, the peak experimental and computational velocities differed by 4% at $t=0.28$, and occurred at normalized radial positions of $+0.35$ and $+0.45$, respectively [Fig. 9(c)]. At the same position and $t=0.73$, the peak experimental and computational velocities differed by 1%, and both occurred at normalized radial positions of $+0.36$

[Fig. 9(d)]. A statistical comparison between the experimentally measured data and computational results for all positions and four time points revealed a correlation coefficient of 0.93.

DISCUSSION

The goal of this study was to gain an understanding of the relative importance of dynamic curvature changes on the flow-induced shear stresses at the walls of coronary arteries. No previous study completely addressed the effects of physiologic (large) curvature changes on coronary artery flow patterns. This study analyzed the flow patterns in individual curved tubes with dynamic and quasistatic variations in curvature using computational methods. The walls of the tubes were assumed to maintain a constant cross section, the prescribed flow rate was steady, and the inlet velocity was assumed to be uniform. An experimental apparatus, employing ultrasonic velocimetry to measure velocity profiles, aided in verifying the results of the computational model.

The overall behavior of flow entering a curved tube with dynamically varying curvature was found to be similar to that of a static curved tube. Initially, the velocity profile was skewed toward the inner wall of curvature. Beyond 2 TDs, the velocity profile was skewed toward the outer wall, and secondary velocities were established that resembled the vortices reported by Dean,[5,6] among others. The experimental results confirmed the overall nature of the computational predictions, with a correlation coefficient of 0.93. The fact that the radial positions of the peak velocities corresponded well may be the best indicator of the agreement. It should be noted that there were several uncertainties associated with the experimental measurements. The most important uncertainties are associated with the use of Doppler ultrasound, and include noise, inaccuracies in determining the angle with respect to the tube axis, and beam alignment in the symmetry plane. A brief analysis of this potential source of error revealed that an error of 5° in the determination of the Doppler angle would result in a 16% change in the peak velocity. This may have been the reason for the larger discrepancies at the 4 TD position. The presence of echoes near the far wall (the inner wall of curvature) made the determination of the wall location difficult. Thus, the experimental verification provides only a general indication of the validity of the computational results.

This study focused mainly on the effects of dynamic curvature variation on the wall shear rates since oscillations in wall shear rate correlate well with sites of intimal thickening in the carotid artery[14] and abdominal aorta.[20] The effect of dynamic curvature change was to increase the mean wall shear rate by as much as 6.7%, relative to the case where the curvature is constant and equal to the mean curvature of the dynamic case. Increases in the mean WSR were noted at the inner, mid and outer walls. These results indicate that the use of a static geometry to predict the mean wall shear rates should yield reasonably accurate results. The error would be similar to that associated with assuming rigid vessel walls and a Newtonian fluid behavior.[10] The quasistatic and dynamic cases were all run at the same converged mesh density and time step. Therefore, differences seen between the quasisteady and dynamic cases were not related to the threshold for grid sensitivity. The differences between the two cases are truly due to the addition of dynamic motion.

The change in curvature also resulted in a variation in wall shear rate over the simulated cardiac cycle. This variation, expressed as the NWSRA, was as much as 52% of the wall shear rate in a static curved tube with the same mean curvature as the dynamic case, with the highest NWSRA occurring at the midwall. These effects may be compared to the effects of including a pulsatile pressure gradient, which is generally regarded as one of the most important factors in determining the flow field. Under normal resting conditions, the pulsatility of the volume flow wave form creates a 100%–150% variation in wall shear rate over the cardiac cycle.[21] Thus, the variation in curvature can create variations in wall shear rate over the cardiac cycle that are similar in magnitude to the variations created by pulsatility. The relative effects of these two factors will also depend on the phase angle between the pressure gradient and the curvature variation. Since phase angle differences in these flow quantities have also been associated with atherosclerosis development,[17] these issues should be addressed in future research.

The finding that dynamic curvature variation increases mean wall shear rate has important implications for predicting areas of the coronary vasculature that may be prone to atherosclerosis development. The inclusion of dynamic geometry may eliminate some areas that would be predicted as having a low mean shear stress by a static analysis. The degree to which these areas would be eliminated would depend on the local curvature and the change in curvature. The effect on the shear rate amplitude might be to increase the degree of shear rate oscillation at the inner walls of curvature. The importance of these effects will also depend on the inclusion of higher frequency components in the geometry variation. In order to accurately compare the wall shear rate distribution to indicators of atherosclerosis development (such as intimal thickening), it is necessary to fully model the dynamic nature of the vessel geometry. This could be done utilizing three-dimensional dynamic geometry data from biplanar angiograms.

Although the computational models used here were up to 32 TDs in length, only the results within the first

10 TDs should be considered as relevant to flow in the coronary arteries. As mentioned earlier, the coronary arteries typically branch every few TDs. The plane and/or direction in curvature may also change within 10 TDs. It is also important to consider the amount of total movement the tube undergoes. For the model constructed here (with a fixed entrance), the highest total displacement of the tube at an axial position of 10 TDs was 11.8 diameters (the total arc length traced by that point on the centerline of the tube over the simulated cardiac cycle) for the case $\delta_m = 0.12$, $\varepsilon = 0.5$. There was an approximately linear correspondence between the total displacement and both δ_m and ε. Previous analysis of angiographic data showed that coronary arteries are displaced as much as 5 diameters.[21] Since the maximum values of the NWSRA occurred within the first 6 TDs for the $\delta_m = 0.12$, $\varepsilon = 0.5$ case, these results should be indicative of physiologic coronary artery flow.

These results may also be compared to the two previously published studies of flow in curved tubes with time-varying curvature. The velocity profile distortions seen in this study were similar to those observed by Schilt et al.,[29] although different values of δ_m and ε were employed. Qualitative agreement with the analytical results of Lynch et al.[18] was observed, but it is important to note that their study was limited to low values of δ_m, ε and α. Their analysis predicted that the wall shear stress amplitude due to dynamic curvature would be on the order of 10^{-3} compared to the presence of curvature alone. The results presented in this study support that conclusion, since the NWSRA were very small (5% or less) for the case closest to their simulations ($\delta_m = 0.03$, $\varepsilon = 0.1$). At the midwall, Lynch et al. predicted a lower axial mean shear stress, and no change in the azimuthal component. In this study, a higher mean shear rate was noted at the midwall. In fact, it was at the midwall where the largest increases in mean wall shear rate were noted. This difference is likely due to the increased movement of the tube associated with the higher values of ε and α used in this study, and less due to the change in curvature itself. It should be noted that since both studies employed the assumption of a Newtonian fluid, the comparison of shear rate to shear stress is valid.

The inclusion of dynamically varying curvature had little effect on the shear rate amplitude for the cases studied here, relative to the quasistatic approach. This may change as more complex geometries (bifurcations, multiplanar curvature, etc.) are included. Furthermore, the curvature in this study was varied sinusoidally in time with a frequency equal to that of the cardiac cycle (1 Hz). Recent data indicate that the variation in curvature over the cardiac cycle is not sinusoidal, and that there are rather swift changes in curvature in systole.[11] Fourier decomposition of the curvature wave forms con-

tained in the work of Gross et al.[11] shows significant components with frequencies of up to 6 Hz (not shown). Increasing the frequency of curvature variation would be expected to significantly increase the shear rate amplitudes reported here.

There may also be important phenomena associated with the solid wall stresses in deforming curved tubes to be considered. One would expect rather large strains to occur in the tube wall when the radius of curvature varies by 80%. The stresses in a simplified model of a deforming coronary artery were the subject of a recent study that also tracked atherosclerotic plaque progression.[31] It was found that stresses were 1.5–1.9 times greater when the flexion angle of a coronary artery model was changed from 10° to 20°. However, the model used to estimate these stresses did not include many of the factors that are known to be important in determining arterial wall stresses, such as nonlinear mechanical properties and residual stresses.[8]

The study of Stein et al.[31] also found that the atherosclerotic plaques in regions where flexion was greatest progressed more rapidly. Angiographic images of coronary arteries were evaluated in 33 patients over a period of approximately 25 months. The progression of an atherosclerotic plaque was expressed as the change in percent stenosis from the initial to the final angiogram. The average angle of flexion in the region of plaques that progressed was 19°, as compared to the average angle of flexion in the region of plaques that did not progress, 9°. Whether the progression is due to fluid or solid mechanical phenomena remains to be determined. It is likely that both affect the process to some degree. While the results of this study indicate that a higher shear rate amplitude (and possibly more shear rate oscillation) might be found if the dynamic curvature is taken into account, the simplifications made in the construction of this model (fixed entrance, uniplanar curvature, etc.) somewhat limit the application to the in vivo situation. Again, this study was initiated to gain a better understanding of the fluid dynamics. It is intended that more physiologic models be constructed in the future.

In summary, a computational model of flow in a curved tube model of the coronary arteries was constructed whose radius of curvature varied with time. While the change of curvature was found to be important based on quasistatic analysis, the dynamic behavior was not found to be significant at the base cardiac frequency of 1 Hz. Future research will be concerned with higher frequency deformation as well as with the inclusion of branch arteries and a pulsatile pressure gradient.

ACKNOWLEDGMENT

REFERENCES

[1] Arteriosclerosis. The National Heart, Lung, and Blood Institute, National Institutes of Health, Report No. 81-2304, 1981.

[2] Austin, L. R., and J. D. Seader. Entry region for steady viscous flow in coiled circular pipes. *AIChE. J.* 20:820–822, 1974.

[3] Batten, J. R., and R. M. Nerem. Model study of flow in curved and planar arterial bifurcations. *Cardiovasc. Res.* 16:178–186, 1982.

[4] Berger, S. A., L. Talbot, and L. S. Yao. Flow in curved pipes. *Annu. Rev. Fluid Mech.* 15:461–512, 1983.

[5] Dean, W. R. Note on the motion of fluid in a curved pipe. *Philos. Mag.* 4:208–223, 1927.

[6] Dean, W. R. The stream-line motion of fluid in a curved pipe. *Philos. Mag.* 5:673–695, 1928.

[7] Delfino, A., J. E. Moore, Jr., and J. J. Meister. Lateral deformation and movement effects on flow through distensible tube models of blood vessels. *Biorheology* 31:533–547, 1994.

[8] Delfino, A., J. E. Moore, Jr., N. Stergiopulos, and J. J. Meister. Residual strain effects on wall stress in a model of the carotid artery. *J. Biomech.* 30:777–786, 1997.

[9] Friedman, M. H., C. B. Bargeron, O. J. Deters, G. M. Hutchins, and F. F. Mark. Correlation between wall shear and intimal thickness at a coronary artery branch. *Atherosclerosis (Berlin)* 68:27–33, 1987.

[10] Friedman, M. H., C. B. Bargeron, D. Duncan, G. M. Hutchins, and F. F. Mark. Effects of arterial compliance and non-Newtonian rheology on correlations between intimal thickness and wall shear. *ASME J. Biomech. Eng.* 114:317–320, 1992.

[11] Gross, M. F., D. B. Vanfossen, and M. H. Friedman. Curvature changes of the left anterior descending coronary artery during the cardiac cycle. In: ASME IMECE Proceedings, Atlanta, edited by S. Rastegar. New York: ASME, 1996, BED Vol. 33.

[12] Grottum, P., A. Svindland, and L. Walloe. Localization of atherosclerotic lesions in the bifurcation of the main left coronary artery. *Atherosclerosis (Berlin)* 47:55–62, 1983.

[13] He, X., and D. N. Ku. Pulsatile flow in the human left coronary artery bifurcation: Average conditions. *ASME J. Biomech. Eng.* 118:74–82, 1996.

[14] Ku, D. N., D. P. Giddens, C. K. Zarins, and S. Glagov. Pulsatile flow and atherosclerosis in the human carotid bifurcation: Positive correlation between plaque location and low and oscillating shear stress. *Arteriosclerosis* 5:293–302, 1985.

[15] Lai, Y. G., A. J. Przekwas, and R. L. Sun. CFD simulation of automotive IC engines with advanced moving grid and multi-domain methods. AIAA 24th Fluid Dynamics Conference, Orlando, 1993.

[16] Lai, Y. G., and A. J. Przekwas. A finite volume method for simulation of fluid flows with moving boundaries. AIAA 32nd Aerospace Sciences Meeting, Reno, 1994.

[17] Lee, C. S., and J. M. Tarbell. Influence of vasoactive drugs on wall shear stress distribution in the abdominal aortic bifurcation: An *in vitro* study. *Ann. Biomed. Eng.* 26:200–212, 1998.

[18] Lynch, D. G., S. L. Waters, and T. J. Pedley. Flow in a tube with non-uniform, time-dependent curvature: Governing equations and simple examples. *J. Fluid Mech.* 323:237–264, 1996.

[19] Mark, F. F., C. B. Bargeron, O. J. Deters, and M. H. Friedman. Nonquasi-steady character of pulsatile flow in human coronary arteries. *ASME J. Biomech. Eng.* 107:24–28, 1985.

[20] Moore, J. E., Jr., C. Xu, S. Glagov, C. K. Zarins, and D. N. Ku. Fluid wall shear stress measurements in a model of the human abdominal aorta: Oscillatory behavior and the relationship to atherosclerosis. *Atherosclerosis (Berlin)* 110:225–240, 1994.

[21] Moore, J. E., Jr., N. Guggenheim, A. Delfino, P. A. Doriot, P. A. Dorsaz, W. Rutishauser, and J. J. Meister. Preliminary analysis of the effects of blood vessel movement on blood flow patterns in the coronary arteries. *ASME J. Biomech. Eng.* 116:302–306, 1994.

[22] Nerem, R. M., and W. A. Seed. Coronary artery geometry and its fluid mechanical implications. In: Fluid Dynamics as a Localizing Factor for Atherosclerosis, edited by G. Schettler. Berlin: Springer, 1983.

[23] Pao, Y. C., J. T. Lu, and E. L. Ritman. Bending and twisting of an *in vivo* coronary artery at a bifurcation. *J. Biomech.* 25:287–295, 1992.

[24] Pedley, T. J. The Fluid Mechanics of Large Blood Vessels. Cambridge: Cambridge University Press, 1980.

[25] Perktold, K., R. M. Nerem, and R. O. Peter. A numerical calculation of flow in a curved tube model of the left main coronary artery. *J. Biomech.* 24:175–189, 1991.

[26] Perktold, K., and G. Rappitsch. Computer simulation of local blood flow and vessel mechanics in a compliant carotid artery bifurcation model. *J. Biomech.* 28:845–856, 1995.

[27] Sabbah, H. N., F. J. Walburn, and P. D. Stein. Patterns of flow in the left coronary artery. *ASME J. Biomech. Eng.* 106:272–279, 1984.

[28] Santamarina, A. Miami, FL: Florida International University, MS Thesis, 1998.

[29] Schilt, S., J. E. Moore, Jr., A. Delfino, and J. J. Meister. The effects of time-varying curvature on velocity profiles in a model of the coronary arteries. *J. Biomech.* 29:469–474, 1996.

[30] Singh, M. P. Entry flow in a curved pipe. *J. Fluid Mech.* 65:517–539, 1974.

[31] Stein, P. D., M. S. Hamid, K. Shivkumar, T. P. Davis, F. Khaja, and J. W. Henry. Effect of cyclic flexion of coronary arteries on progression of atherosclerosis. *Am. J. Cardiol.* 73:431–437, 1994.

[32] Tang, T. D., D. P. Giddens, C. K. Zarins, and S. Glagov. Velocity profile and wall shear measurements in a model human coronary artery. In: ASME Winter Annual Meeting Proceedings, Atlanta. New York: ASME, 1991, BED Vol. 24.